The stability of an evaporating liquid surface

Andrea Prosperetti

Dipartimento di Fisica, Università degli Studi, Milano, 20133 Italy

Milton S. Plesset

California Institute of Technology, Pasadena, California 91125 and University of California, Los Angeles, California 90024

A linearized stability analysis is carried out for an evaporating liquid surface with a view of understanding some observations with highly superheated liquids. The analytical results of this study depend on the unperturbed temperature near the liquid surface. The absence of this data renders a comparison with experiment impossible. However, on the basis of several different assumptions for this temperature distribution, instabilities of the interface of a rapidly evaporating liquid are found for a range of wavenumbers of the surface wave perturbation. At large evaporating mass flow rates the instability is very strong with growth times of a millisecond or less. A discussion of the physical mechanism leading to the instability is given.

I. INTRODUCTION

The safety of light-water cooled nuclear power plants has increased interest in the effects that take place when water at high temperature and pressure is suddenly exposed to a very low pressure. Such a situation would conceivably occur in the so-called loss-of-coolant accident in which there is a break in the boundary of the nuclear system. Such a break would expose water at a temperature near 600 °F and at a pressure of the order of 2200 psi to the low ambient containment pressure. The simplest experimental condition in which these effects can be studied, usually referred to as "Standard Problem No. 1," is that of a long straight pipe filled with high-temperature, high-pressure water, one end of which is suddenly exposed to atmospheric pressure by bursting a diaphragm (see, e.g., Edwards and O'Brien[1]) or by fast-opening devices (see, e.g., Lienhard *et al.*[2]). In this kind of experiment one observes violent boiling of the liquid occurring at and below the free surface and on the walls of the pipe, which causes the liquid to be ejected from the pipe.

An experiment of similar nature with water and other liquids was performed on a smaller scale by Fauske and Grolmes[3] who quickly exposed superheated liquids to a large low-pressure volume. Because of the smaller scale and the cleanliness of the apparatus, boiling (either in the bulk of the liquid or at the walls of the container) was not observed in these experiments. Rather, Fauske and Grolmes observed that above a certain superheat characteristic of the system the liquid free surface quickly broke up with the ejection of a large number of droplets. This droplet ejection gives a mass flux many orders of magnitude greater than that characteristic of ordinary evaporation. Fauske and Grolmes also noted that during the ejection process the pressure in the liquid away from the interface was much greater than that in the low-pressure reservoir to which the liquid was exposed.

These observations can be understood by supposing that the interface between the evaporating liquid and the vapor becomes unstable with a consequent ejection of drops which leaves fresh liquid surface behind, which in its turn becomes unstable. It is this possibility that we propose to investigate in the present paper by considering the stability of the surface of a superheated liquid undergoing fast evaporation. It is probable that such an instability would play a role also in the experiments on Standard Problem No. 1 previously referred to, although the presence of internal boiling in them complicates the analysis substantially. A possibility mentioned by Hooper and Luk[4] is that the surface instability evolves into a crater which closes off, becoming a bubble, which then bursts upon growth, thus shedding droplets. This hypothesis would explain the large number of surface bubbles observed in these circumstances.

It has been known for some time in the chemical engineering literature that an evaporating liquid surface can develop ripples and corrugations which enhance the evaporation process.[5-7] These studies, however, did not indicate the ejection of droplets from the interface. Most likely the reason for this is the lower range of superheats which has been examined. The formation of droplets has not been unequivocally observed, but is strongly suggested by indirect evidence in the experiments of Shepherd and Sturtevant[8] who observed the rapid evaporation of drops in a host liquid near the superheat limit.

Of the available analyses of the stability of an evaporating surface, one[9] does not appear to exhibit the correct behavior in the inviscid limit and, due to other assumptions, is of limited validity. The other theoretical studies do not develop values of the growth rates of instabilities as will be done in the present study. Rather, they are concerned with the conditions of marginal stability under the assumption that they would correspond to a time independence of the perturbation. It will be shown below that this assumption may not be verified in the situation of present concern.

A familiar source of perturbation of an interface are flows induced by surface tension gradients. These Marangoni effects are characterized by a time scale much slower than that of interest here, as will be obvious from the results to be obtained, and therefore will not be considered. Clearly, since surface tension forces tend to inhibit the formation of droplets, the stresses of concern in the present problem are

much higher than those caused by surface tension and surface tension variations.

II. MATHEMATICAL FORMULATION

The situation we envisage here is that of a liquid of infinite extent undergoing steady evaporation from its plane interface. The question to be addressed is that of the stability of this process when the interface is perturbed. To set up a mathematical model for this situation we take the liquid and its vapor to be incompressible inviscid fluids of unlimited extent. *A priori* the effects of compressibility in the vapor may be of some significance not because of flow velocities, which are small, but because of density variations associated with temperature changes. A discussion of this point is deferred until the end of this section.

The neglect of viscosity eliminates one of the destabilizing mechanisms which is thought to be operative at very short wavelengths.[10,11] However, it is not expected to affect significantly phenomena occurring at longer wavelengths, except for a slight damping of the surface perturbation which can be accounted for approximately, as will be seen in Sec. VIIA. It is sometimes stated (see, e.g., Ref. 12, Sec. II) that the motion of a frictionless fluid is also necessarily adiabatic. This is certainly true in principle, and especially for a gas for which the Prandtl number is close to 1. However, in setting up an approximate mathematical model, the guiding principle should not be the relative magnitudes of the thermal diffusivity and kinematic viscosity, but rather the magnitude of the *terms* which involve these parameters relative to other terms in the energy and momentum equations. If an analysis of the orders of magnitude of these terms is carried out, it is found that treating a fluid as inviscid but heat conducting is justified in many cases, including the present one.

We shall append subscripts l and v to quantities pertaining to the liquid and the vapor phase, respectively. No subscripts appear in equations and expressions valid for both fluids. Perturbations will be denoted by a prime, and surface quantities by the subscript s.

For incompressible, inviscid fluids the conservation equations for mass, momentum, and energy are

$$\nabla \cdot \mathbf{u} = 0 , \tag{1}$$

$$\frac{\partial \mathbf{u}}{\partial t} + \mathbf{u} \cdot \nabla \mathbf{u} = -\frac{1}{\rho} \nabla p + \mathbf{g} , \tag{2}$$

$$\frac{\partial T}{\partial t} + \mathbf{u} \cdot \nabla T = D \nabla^2 T . \tag{3}$$

Here $\mathbf{u}$, p, and T denote the velocity, pressure, and temperature fields, ρ is the density, D is the thermal diffusivity, and $\mathbf{g}$ is the acceleration of gravity. The vertical coordinate z is taken to be directed from the liquid into the vapor against gravity. It is convenient to use a frame of reference in which the unperturbed interface is the plane $z = 0$. In this frame the liquid is moving toward the free surface at a velocity W_l. If this velocity is not constant in time, the frame is noninertial and the magnitude of $\mathbf{g}$ can be adjusted to account for this effect if so desired.

Across the interface we must require conservation of mass, normal momentum, and energy, which are expressed by[13–15]

$$J = \rho_l (\mathbf{u}_l - \mathbf{v}) \cdot \mathbf{n} = \rho_v (\mathbf{u}_v - \mathbf{v}) \cdot \mathbf{n} , \tag{4}$$

$$J (\mathbf{u}_v - \mathbf{u}_l) \cdot \mathbf{n} + p_v - p_l = -\zeta \nabla \cdot \mathbf{n} , \tag{5}$$

$$J \{ L + \tfrac{1}{2} [(\mathbf{u}_v - \mathbf{v}) \cdot \mathbf{n}]^2 - \tfrac{1}{2} [(\mathbf{u}_l - \mathbf{v}) \cdot \mathbf{n}]^2 \}$$
$$+ (K_l \nabla T_l - K_v \nabla T_v) \cdot \mathbf{n} = 0 . \tag{6}$$

Here $\mathbf{v}$ is the velocity of the interface, $\mathbf{n}$ is the unit normal directed into the vapor, ζ is the surface tension coefficient, L is the latent heat, K is the thermal conductivity, and J is the mass flux. The first two equations, aside from the surface tension term, appear in an identical form in shock wave theory (Ref. 12, Chap. IX). In the energy equation (6) a small surface-entropy term has been neglected. Furthermore, the kinetic energy terms in the curly brackets are usually much smaller than L so that we have approximately

$$JL + (K_l \nabla T_l - K_v \nabla T_v) \cdot \mathbf{n} = 0 . \tag{7}$$

In this form the equation expresses the fact that the thermal energy conducted to the interface from the liquid side is in part conducted away into the vapor and in part used to effect the change of phase. A similar equation is also encountered in other branches of fluid mechanics as, for example, in thin-flame theory (Ref. 12, Chap. XIV). A further condition arises from the conservation of momentum tangential to the interface. In general this condition is expressed by (see, e.g., Ref. 12, Chap. VII; Ref. 16, Chap. VII; Ref. 15)

$$J \mathbf{n} \times (\mathbf{u}_v - \mathbf{u}_l) + \mathbf{n} \times (\tau_l - \tau_v) \cdot \mathbf{n} = -\mathbf{n} \times \nabla \zeta , \tag{8}$$

where τ denotes the viscous stress tensor. The term in the right-hand side is the tangential surface tension force caused by surface temperature variations. That this effect can induce fluid motion and perturb the plane interface is well-known.[16–19] However, as already indicated in Sec. I, the associated flows do not exhibit the very violent features of the surface disruptive phenomena of present concern. Furthermore, as will be seen from the numerical results to be presented below, they occur on a time scale much slower than the one predicted by our stability analysis. In addition, it will be seen in the following that usually the interface remains relatively isothermal. For all these reasons we feel justified in neglecting surface tension gradient effects as represented by the term in the right-hand side of (8). Since we have also neglected viscosity, the presence of a nonzero mass flux across the interface Eq. (8) can only be satisfied by requiring

$$\mathbf{n} \times (\mathbf{u}_v - \mathbf{u}_l) = 0 , \tag{9}$$

i.e., continuity of the tangential velocity. The effect of this condition is to induce a "refraction" of the streamlines at the interface and to generate vorticity in the fluids. It may be remarked that Eq. (9) is also well known in shock wave theory and combustion phenomena.

Two additional boundary conditions are required to close the system. The first one is the continuity of temperature at the interface,

$$T_l = T_v = T_s . \tag{10}$$

The second one is not so straightforward and warrants some discussion.

One possibility to close the system is to use a relation connecting the mass flux J at the interface to the local temperature T_s,[10]

1591   Phys. Fluids, Vol. 27, No. 7, July 1984

A. Prosperetti and M. S. Plesset   1591

$$J = J(T_s) . \tag{11}$$

An explicit example of such a relation is given by the well-known Hertz–Knudsen equation[20,21]

$$J = \alpha (RT_s/2\pi M)^{1/2} \left[\rho_v^e(T_s) - \rho_v \right] . \tag{12}$$

Here R and M denote the universal gas constant and the molecular weight of the vapor and the superscript e indicates the equilibrium value along the saturation line. The parameter α is the accommodation coefficient for condensation and evaporation which, for simple liquids, is close to 1. When there is a net flux (i.e., $J \neq 0$), transport theory indicates that a numerical factor of order 2 should be introduced in Eq. (12) to multiply the right-hand side.[21,22] This matter appears to be somewhat controversial at present,[23] but in any case the value of α can be adjusted to incorporate this correction. In the numerical examples to be shown below we shall take $\alpha = 1$ and it will be seen that different values of this quantity would have only very minor effects.

If T_s and ρ_v undergo small changes T_s' and ρ_v' the variation J' in mass flux predicted by Eq. (12) is

$$J' = \alpha \left(\frac{RT_s}{2\pi M} \right)^{1/2} \left[\left(\frac{1}{2T_s} (\rho_v^e - \rho_v) + \frac{d\rho_v^e}{dT} \right) T_s' - \rho_v' \right] .$$

For many liquid–vapor systems, including water, the numerical value of $d\rho_v^e/dT$ in the temperature range of practical interest is such that the last term in this relation is negligible with respect to the second one. It is therefore reasonable to retain the dependence of J on T_s only, as indicated in Eq. (11), consistently with the neglect of variations in the vapor density.

If we had allowed the vapor to be compressible, an alternative procedure to the use of Eq. (11) would be to impose thermodynamic equilibrium at the interface in the form

$$p_v = p_v^e(T_s) , \quad \rho_v = \rho_v^e(T_s) . \tag{13}$$

Since we have taken ρ_v to be constant, we could use the first of these relations dropping the second one. This procedure has been followed in the literature as, for example, by Hsieh.[14] In the present study we shall follow the first approach, mainly, and in one example we shall compare those results with the ones given by the second procedure. From this comparison it will be seen that the two approaches do not lead to large differences, a behavior which implies that the effects of thermodynamic nonequilibrium are small.

In summary, the mathematical formulation of the problem at hand consists of the field equations (1)–(3), to be satisfied in the liquid and in the vapor, and of the boundary conditions (4), (5), (9), (10), and (11) or the first of (13).

We wish to comment briefly on the effect of compressibility in the continuity equation (1). The complete form of this equation would be

$$\left(\frac{\partial \rho_v}{\partial p} \right)_T \frac{dp}{dt} + \left(\frac{\partial \rho_v}{\partial T} \right)_p \frac{dT}{dt} + \rho_v \nabla \cdot \mathbf{u}_v = 0 ,$$

where d/dt indicates the convective derivative. The first two terms, which are absent from our Eq. (1), will affect both the unperturbed situation of steady evaporation from a plane interface and the development of the perturbation caused by the interfacial wave. As for the first point, Plesset[24] has shown that, in the conditions of present concern, all the

fields are very nearly uniform near the evaporating surface so that the equation is trivially satisfied either with or without the first two terms. As far as the perturbation is concerned, we may note that the ratio of the second to the first term may be estimated to be of the order

$$\left(\frac{\partial \rho_v}{\partial T} \right)_p \frac{dT}{dt} \left[\left(\frac{\partial \rho_v}{\partial p} \right)_T \frac{dp}{dt} \right]^{-1} \simeq \left(\frac{\partial p}{\partial T} \right)_\rho \frac{T'}{p'} ,$$

which, for a perfect gas, equals pT'/Tp'. As will be clear from the following, for the type of flow considered here, the source of the perturbation is at the free surface, and the perturbations themselves decay away from the interfacial region. It is therefore reasonable to estimate the magnitude of T'/p' by means of the Clausius–Clapeyron relation to find

$$\left(\frac{\partial p}{\partial T} \right)_\rho \frac{T'}{p'} \simeq \frac{RT}{ML} .$$

The quantity on the right-hand side is usually small (e.g., equal to 0.076 for water at 100 °C), and hence density variations due to temperature variations are seen to be small in comparison with those due to pressure perturbations, and these are negligible here due to the assumed slow velocities. It should be stressed that this estimate depends critically upon the Clausius–Clapeyron equation which can be applied in view of the fact that perturbations are generated at the interface, and that conditions are not too different from thermodynamic equilibrium in its neighborhood.

III. THE UNPERTURBED STATE

In the unperturbed state the liquid–vapor interface, which is located at $z = 0$, is plane and evaporation is taking place with the liquid approaching the interface from the region $z < 0$ with velocity W_l and the vapor leaving it with velocity W_v. It is known[24,25] that in the presence of any appreciable evaporative flux the temperature gradient in the vapor is very nearly zero, so that the pertinent form of the mass and energy relations (4) and (7) at the interface is

$$J = \rho_l W_l = \rho_v W_v , \tag{14}$$

$$LJ = K_l G_l , \tag{15}$$

where G_l denotes the negative of the undisturbed liquid temperature gradient at the interface.

The method of solution which will be adopted here is that of the separation of the time variable, or normal-mode analysis. In order for this method to be mathematically exact the unperturbed state must be independent of time. However, the steady solution of the energy equation (3) in the liquid satisfying $T = T_s$ and $dT/dz = -G_l$ at $z = 0$ is given by

$$T_l = T_s + (D_l G_l/W_l) \left[1 - \exp(W_l z/D_l) \right] . \tag{16}$$

Letting $z \to -\infty$ and using (15), we obtain from this equation

$$T_\infty - T_s = L/c_{pl} , \tag{17}$$

where c_{pl} is the liquid specific heat, independent of the evaporation rate. [This relation expresses the fact that, for each liquid layer, the latent heat required for evaporation is entirely supplied by a loss $c_{pl}(T_\infty - T_s)$ of the liquid enthalpy.] The value of L/c_{pl} for most liquids is quite large (e.g., of the

order of 600 K for water far from the critical point), and the subcooling indicated by (17) is quite unrealistic. The implication is that a steady temperature distribution in an evaporating quiescent unbounded liquid is not a physical possibility. The evaporation rate of such a liquid exposed to a pressure lower than saturation is bound to decrease in time, at least until possible boundary effects, such as heat flux from the bottom of the container, begin to make themselves felt.

In the presence of such a time-developing unperturbed base state the normal-mode analysis to be carried out below retains only an approximate validity to the extent that the predicted time scale for the development of the surface instability is much shorter than that for the evolution of the unperturbed state. A similar approximation has been followed for many years in other areas such as natural convection research (see, e.g., Ref. 26). The full time-dependent problem here appears to require a numerical treatment already for the unperturbed state since W_l, which enters in the energy equation, depends on the solution to this equation through the boundary conditions. Such an analysis would be premature without a preliminary understanding of the physical mechanisms underlying the instability of present concern which is the principal objective of the present study. These considerations motivate our choice of carrying out this analysis with the assumption that an unperturbed temperature profile in the liquid, possibly depending parametrically on time, $T_l(z,t)$, is given. A time variation of the surface gradient and hence, by (15), of the evaporation rate entails a similar variation of the velocity fields W_l and W_v. Again, we shall treat them as constants in space and time thus assuming in effect that any such variations are sufficiently slow.

The last aspect of the unperturbed state that remains to be specified is the pressure field in the liquid and in the vapor. With the neglect of inertial effects due to time dependence of the mass flux, we have the hydrostatic relations

$$P_l = P_{sl} - \rho_l g z , \quad P_v = P_{sv} - \rho_v g z , \tag{18}$$

where $g = |\mathbf{g}|$. Although we shall not consider explicitly the Rayleigh–Taylor unstable configuration in which the liquid lies above the vapor we may remark that our results apply also to this case if the sign of g is reversed.

It is of interest to observe that the pressure acting on the liquid at the interface, P_{sl}, exceeds that in the vapor, P_{sv}, by an amount specified by the momentum boundary condition (5),

$$P_{sl} = P_{sv} + J^2(1/\rho_v - 1/\rho_l) . \tag{19}$$

This effect is caused by the expansion of the fluid particles undergoing the transition from the liquid to the vapor state so as to "push back" on the liquid. Note that this effect does not change sign for condensation. In this case the increase in liquid pressure arises because the vapor is very nearly stopped at the interface. Our results are not directly applicable to this case, however, due to the neglect of the temperature gradient in the vapor which is important for condensation.

IV. THE PERTURBATION PROBLEM

A perturbation is now introduced in the system in the form of a surface wave with wavenumber k given by

$z = \eta(x,y,t)$ with

$$\eta = a(t)f(x,y) . \tag{20}$$

For our purposes the function $f(x,y)$ need not be specified further than requiring it to be a solution of

$$\left(\frac{\partial^2}{\partial x^2} + \frac{\partial^2}{\partial y^2} + k^2\right)f = 0 , \tag{21}$$

bounded at infinity in the (x,y) plane. Upon subtraction of the unperturbed component and linearization, the field equations (1)–(3) require that the perturbation fields, denoted by a prime, satisfy

$$\nabla \cdot \mathbf{u}' = 0 , \tag{22}$$

$$\frac{\partial \mathbf{u}'}{\partial t} + W \frac{\partial \mathbf{u}'}{\partial z} = -\frac{1}{\rho} \nabla p' , \tag{23}$$

$$\frac{\partial T'}{\partial t} + W \frac{\partial T'}{\partial z} + \mathbf{u}' \cdot \nabla T = D \nabla^2 T' . \tag{24}$$

The boundary conditions (4), (5), (7), (9), (10), (11) can be put in the form

$$J' = \rho_l\left(w_l' - \frac{\partial \eta}{\partial t}\right) = \rho_v\left(w_v' - \frac{\partial \eta}{\partial t}\right) , \tag{25}$$

$$p_l' = p_v' + 2(W_v - W_l)J' + [(\rho_l - \rho_v)g + \zeta k^2]\eta , \tag{26}$$

$$LJ' + K_l\left(\frac{\partial T_l'}{\partial z} + \eta \frac{\partial^2 T_l}{\partial z^2}\right) - K_v \frac{\partial T_v'}{\partial z} = 0 , \tag{27}$$

$$\mathbf{n} \times (\mathbf{u}_v' - \mathbf{u}_l') = 0 , \tag{28}$$

$$T_l' = T_v' = T_s' , \tag{29}$$

$$J' = \frac{\partial J}{\partial T_s} T_s' . \tag{30}$$

Equation (29) must be imposed at $z = \eta$, whereas the remaining four have been written in a form allowing them to be imposed on $z = 0$ to first order in η. In Eq. (25), w' indicates the z component of the perturbation velocity $\mathbf{u}'$.

A consideration of the momentum boundary condition (26) is particularly illuminating. In the absence of a mass flux the normal pressure pattern of surface waves prevails, with p_l' positive under the (liquid) crests and negative under the (liquid) troughs and vice versa for p_v'. This pressure distribution generates the motion of the liquid from the crests to the troughs and of the vapor in the opposite direction. If the system is unstable, this pressure must be reversed and p_l' has to become *negative* under the crests so as to make them grow. Since the last term in (26) is obviously positive for a crest, this result can only be obtained if the second term becomes negative through a decrease of the flux on the crests (i.e., $J' < 0$ when $\eta > 0$). The physical mechanism at work in this case can be illustrated with reference to Fig. 1. The reduced evaporation rate on the crests has the effect of partially relieving the vapor back pressure on the liquid. The converse takes place at the troughs where the pressure is increased due to the greater evaporation. The incoming liquid streamlines are then deflected as shown, and more liquid goes to feed the growing crests. *A priori* an instability could also occur if p_v' were large and negative. That the instability be driven by phenomena occurring in the vapor would be rather surprising, and indeed we have found no evidence of this occurrence in the numerical results.
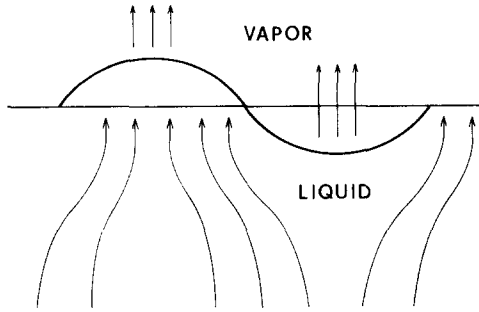
1593   Phys. Fluids, Vol. 27, No. 7, July 1984

A. Prosperetti and M. S. Plesset   1593

$$\varphi_l = \Phi_l e^{kz} f(x,y) , \tag{31}$$

where Φ_l is a constant amplitude. The exponential time factor will be understood here and in the sequel. The velocity field in the vapor is on the other hand rotational and is given by

$$\mathbf{u}_v' = A_v \mathbf{K} + \nabla \times (B_v \mathbf{K}) + \nabla \varphi_v , \tag{32}$$

where $\mathbf{K}$ is a unit vector in the positive z direction and A_v, B_v are scalar functions of positions and time related to the vorticity field. It will be shown in the Appendix that, as a consequence of the requirement of continuity of the tangential velocity, one finds $B_v = 0$. The z component of the velocity $\mathbf{u}_v'$ is then given by

$$w_v' = [k^2 W_v^2/(k^2 W_v^2 - \sigma^2)]\alpha_v \exp(-\sigma z/W_v)f$$
$$+ k\{[W_v/(\sigma - kW_v)]\alpha_v - \Phi_v\} e^{-kz} f, \tag{33}$$

where α_v and Φ_v are constants, the first of which is the vorticity amplitude since the vorticity field in the vapor is given by

$$\boldsymbol{\omega}_v = \alpha_v \exp(-\sigma z/W_v)\nabla \times (\mathbf{K} f) . \tag{34}$$

We note that boundedness at infinity is reconcilable with the last two equations if and only if Re $\sigma > 0$, that is, only for unstable (or neutrally stable) modes. Solutions in the stable case have a different structure, with vorticity confined in the liquid (see, for a similar situation, Ref. 12, p. 478). In the liquid the pressure field is given by $p_l' = \Pi_l e^{kz} f$, where

$$\Pi_l = -\rho_l(\sigma + kW_l)\Phi_l , \tag{35}$$

whereas in the vapor we find $p_v' = \Pi_v e^{-kz} f$ with

$$\Pi_v = \rho_v [(kW_v - \sigma)\Phi_v + \tfrac{1}{2}\alpha_v W_v] . \tag{36}$$

At this point the boundary conditions on mass, normal momentum, and tangential velocity can be imposed to express $\Phi_{l,v}$ and α_v in terms of the wave amplitude a. The result is

FIG. 1. Qualitative illustration of the mechanism causing the surface instability, seen from a frame of reference in which the undisturbed evaporating surface is at rest. The evaporating mass flux is increased at the (liquid) troughs and decreased at the (liquid) crests. As a consequence the "backpush" of the departing vapor on the liquid is greater at the troughs than at the crests. The associated pressure gradient drives the liquid towards the crests causing their growth and the amplification of the surface deformation.

We now proceed directly to show the solution of the perturbed problem and the characteristic equation and to discuss some illustrative results. Details of the solution procedure are provided in the Appendix.

V. SOLUTION

According to the normal mode procedure we postulate for all perturbation quantities a time dependence proportional to exp (σt). With this assumption the field equations can be solved in the manner detailed in the Appendix in terms of surface amplitudes of the various fields which are to be determined from the boundary conditions. The growth rate σ is then obtained as a condition of solvability of the resulting linear homogeneous system.

The velocity field in the liquid is found to be irrotational and derivable from a potential, $\mathbf{u}_l' = \nabla \varphi_l$, with

$$\Phi_l = \frac{(\rho_l - \rho_v)(\sigma^2 + 2kW_v\sigma + k^2 W_l W_v) - (\rho_l + \rho_v)\omega_0^2}{2k\rho_l(\sigma + kW_v)} a , \tag{37}$$

$$\Phi_v = \frac{(\rho_l^2 - \rho_v^2)(\sigma^2 + \omega_0^2) - k^2 W_l W_v(\rho_l - \rho_v)(3\rho_l - \rho_v)}{4k\rho_l\rho_v(\sigma + kW_v)} a , \tag{38}$$

$$\alpha_v = -\frac{(\rho_l - \rho_v)^2(\sigma^2 + k^2 W_l W_v) + (\rho_l + \rho_v)^2\omega_0^2}{2k\rho_l J} a , \tag{39}$$
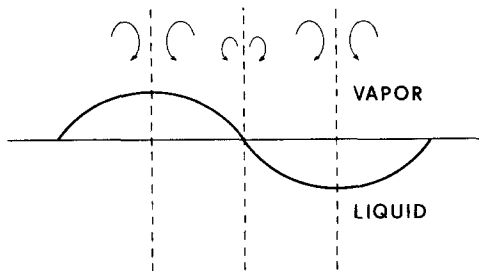

FIG. 2. Qualitative illustration of the vorticity pattern in the vapor over the surface wave in the unstable case. The liquid motion is irrotational.

where we have introduced the natural frequency of ordinary surface waves, ω_0, given by

$$\omega_0^2 = [(\rho_l - \rho_v)/(\rho_l + \rho_v)] gk + [\zeta/(\rho_l + \rho_v)] k^3 . \tag{40}$$

It is interesting to note that α_v/a is negative definite. From the expression (34) of the vorticity field it can be inferred that the vorticity distribution in the vapor above the wave has the character sketched in Fig. 2, with the rotational velocity component decreasing the velocity on crests and increasing it on troughs. This result is in agreement with what can be expected from a consideration of the term $\nabla \rho \times \nabla p$ of the vorticity equation. At the interface (which we can view for a

moment as a region of small but finite thickness across which the density undergoes a rapid change) $\nabla\rho$ is directed from the vapor into the liquid and ∇p from the crests to the troughs in the unstable case.

Equations (37)–(39) enable us to compute other interesting quantities such as the perturbations in the mass flux J',

$$J' = -\frac{(\rho_l + \rho_v)(\sigma^2 + \omega_0^2) + kJ[2\sigma - k(W_v - W_l)]}{2(\sigma + kW_v)} a, \tag{41}$$

the pressure amplitudes,

$$\begin{aligned}\Pi_l = &-(\sigma + kW_l)/2k(\sigma + kW_v)\\ &\times[(\rho_l - \rho_v)(\sigma^2 + 2kW_v\sigma + k^2W_lW_v)\\ &-(\rho_l + \rho_v)\omega_0^2]a,\end{aligned} \tag{42}$$

$$\begin{aligned}\Pi_v = &-[2k(\sigma + kW_v)]^{-1}\\ &\times\{(\rho_l - \rho_v)\sigma^3 - kW_l(\rho_l - \rho_v)\sigma^2\\ &+[(\rho_l\rho_v)\omega_0^2 - k^2J(W_v - W_l)]\sigma\\ &+(\rho_l + \rho_v)kW_l\omega_0^2\\ &+k^3J(W_v - W_l)(2W_v - W_l)\}a,\end{aligned} \tag{43}$$

and the vapor velocity at the interface

$$w_z'|_{z=0} = -\frac{(\rho_l - \rho_v)(\sigma^2 - k^2W_lW_v) + (\rho_l + \rho_v)\omega_0^2}{2\rho_v(\sigma + kW_v)}a. \tag{44}$$

We may note in passing that, setting $J' = 0$ as would be appropriate for a thin flame on the surface of a liquid fuel, we obtain for σ the same characteristic equation as given by Landau[27] in his classical analysis of the combustion problem (see also Ref. 12, p. 478). The vorticity pattern of Fig. 2 is also applicable to that problem.

The perturbed temperature fields in the liquid and in the vapor have a rather complex form given in full in the Appendix. Here we give only the expressions of the perturbed gradients at the interface in the liquid

$$\mathbf{n}\cdot\nabla T_l' = \mu_l\Theta + \mu_l G_l a - (kG_l/W_l)I_l\Phi_l, \tag{45}$$

and in the vapor

$$\mathbf{n}\cdot\nabla T_v' = -\mu_v\Theta. \tag{46}$$

Here Θ denotes the (common) temperature perturbation at the interface (not at $z = 0$), and μ_l and μ_v stand for

$$\mu_l = \left[\left(\frac{W_l}{2D_l}\right)^2 + k^2 + \frac{\sigma}{D_l}\right]^{1/2} + \frac{W_l}{2D_l}, \tag{47}$$

$$\mu_v = \left[\left(\frac{W_v}{2D_v}\right)^2 + k^2 \frac{\sigma}{D_v}\right]^{1/2} - \frac{W_v}{2D_v}. \tag{48}$$

The last term in (45) accounts for the effect of the distortion of the unperturbed temperature field caused by the liquid motion as can be seen from the definition of I_l which is given by

$$I_l = \frac{W_l}{D_l}\int_{-\infty}^{0}\exp[(k - \mu_l')z]\frac{\partial T/\partial z}{\partial T/\partial z|_0}dz, \tag{49}$$

where

$$\mu_l' = \frac{W_l}{2D_l} - \left[\left(\frac{W_l}{2D_l}\right)^2 + k^2 + \frac{\sigma}{D_l}\right]^{1/2}. \tag{50}$$

We may note that, using the definition of diffusivity in terms of conductivity, density, and heat capacity, with the aid of the boundary condition (15), the expression for I_l can be written

$$I_l = \int_{-\infty}^{0}\exp[(k - \mu_l')z]\frac{\partial\mathrm{Ja}}{\partial z}dz,$$

where

$$\mathrm{Ja}(z) = (c_{pl}/L)[T_\infty T_l(z)]$$

is the local Jacob number. The magnitude of L/c_{pl} tends to make Ja small in most applications although the derivative of this quantity is not necessarily small.

Equations (41), (45), and (46) can now be substituted into the energy boundary condition (27) to express the perturbed surface temperature in terms of the surface elevation a. The result may be written in the form

$$\Theta = \frac{L}{2(\sigma + kW_v)(K_l\mu_l + K_v\mu_v)}S_1(\sigma)a, \tag{51}$$

where

$$\begin{aligned}S_1(\sigma) = &[\rho_l(1 + I_l) + \rho_v(1 - I_l)]\sigma^2\\ &+2k[J + \rho_l(W_v - W_l)I_l]\sigma\\ &+(1 - I_l)[(\rho_l + \rho_v)\omega_0^2 - k^2J(W_v - W_l)]\\ &-2(\sigma + kW_v)J\left(\mu_l + \frac{1}{G_l}\frac{\partial^2 T_l}{\partial z^2}\bigg|_0\right).\end{aligned} \tag{52}$$

VI. THE CHARACTERISTIC EQUATION

The characteristic equation for the determination of σ can be obtained by observing that another relation between Θ and a can be derived from the last boundary condition (30) which involves the surface temperature variation and the perturbed mass flow, Eq. (41). In this way, requiring the two expressions for Θ to coincide, we obtain the characteristic equation in the form

$$S_1(\sigma) - S_2(\sigma) = 0, \tag{53}$$

where

$$\begin{aligned}S_2 = &-\frac{K_l\mu_l + K_v\mu_v}{L\,\partial J/\partial T_s}\\ &\times\{(\rho_l + \rho_v)(\sigma^2 + \omega_0^2) + kJ[2\sigma - k(W_v - W_l)]\},\end{aligned} \tag{54}$$

and S_1 is given by (52). The coefficient multiplying the curly brackets in this expression is usually rather small because the latent heat L is a large quantity. For example, using the estimates $\mu_l \sim W_l/D_l$ and $\partial J/\partial T_s \sim a(RT_s/2\pi M)^{1/2} dp_v^e/dT$ and assuming $K_v\mu_v \ll K_l\mu_l$, for water at 100 °C we find $K_l\mu_l(L\,\partial J/\partial T_s) \sim 4\times10^{-3}W_l$, approximately, where W_l is in cm/sec. Hence it is seen that a good approximation to the characteristic equation (53) is given by

$$S_1(\sigma) \simeq 0, \tag{55}$$

which, as is clear from (51), is the result that one would get substituting for the last boundary condition relating surface

temperature and mass flux the simpler requirement of zero variation of the surface temperature,

$$T'_s = 0 . \tag{56}$$

The nature of the roots of the characteristic equation is therefore really determined by the function S_1, with S_2 providing only a small correction to the values given from the approximation (55). This remark also shows that the actual value of $\partial J / \partial T_s$, and in particular the effect of the accommodation coefficient, can only have a limited influence on the numerical values of σ.

The form of the function S_2 is different if the thermodynamic equilibrium approximation expressed by the first of (13) is used to close the system. In this case Eq. (30) would be replaced by

$$p'_v = \frac{dp^e_v}{dT_s} T'_s + \rho_v g\eta . \tag{57}$$

From this equation we can again obtain an expression for Θ in terms of a using (43). Equating this result to (51), we obtain a characteristic equation of the same form as (53), where now the function S_2 is given by

$$S'_2 = \frac{k_l \mu_l + K_v \mu_v}{2L \, dp^e_v/dT_s} \{ (\rho_l - \rho_v)(2W_v + W_l)\sigma^2$$
$$+ 2\sigma [kJ(W_v - W_l) - (\rho_l + \rho_v)\omega^2_0/k - \rho_v g]$$
$$- \omega^2_0 W_l(\rho_l + \rho_v) - k^2 J(W_v - W_l)$$
$$\times (2W_v - W_l) - 2kgJ \} . \tag{58}$$

One readily finds that the order of magnitude of this function is also small compared with that of S_1.

We should recall that, due to the assumption $\mathrm{Re} \, \sigma \geqslant 0$ made in obtaining S_1, only roots of (53) having a positive real part are acceptable.

VII. RESULTS

In order to illustrate numerically the theoretical results, we need to make a definite choice for the unperturbed temperature distribution in the evaporating liquid. This temperature distribution enters into the characteristic equation through the integral I_l and through the ratio of the second to the first spatial derivative at the interface. We shall consider three different examples which are representative of the possible cases. It will be seen that, although the quantitative predictions do depend on this unperturbed temperature distribution, the qualitative ones do not. In all the computations the physical properties of water at 100 °C have been used.

A. Approximation by integration by parts

Upon integration by parts, the expression (49) for I_l may be written

$$I_l = \frac{W_l}{D_l(k - \mu'_l)} \left[1 + \frac{1}{G_l(k - \mu'_l)} \right.$$
$$\left. \times \left(\frac{\partial^2 T_l}{\partial z^2} \bigg|_0 - \int_{-\infty}^0 \exp\left[(k - \mu'_l)z \right] \frac{\partial^3 T_l}{\partial z^3} \, dz \right) \right] . \tag{59}$$

The process can be continued to obtain an asymptotic expansion of I_l in inverse powers of $(k - \mu'_l)$. For sufficiently large values of k we can evaluate I_l approximately by dropping the integral term in this expression. The same result would be obtained by assuming a parabolic temperature distribution in the liquid near the free surface. This procedure is often followed in heat transfer problems treated by the integral method (see, e.g., Ref. 28). In order to estimate the ratio of the second to the first spatial derivative we note that, from the unperturbed energy equation in the liquid, we obtain

$$\frac{1}{G_l} \frac{\partial^2 T_l}{\partial z^2} \bigg|_0 = - \frac{W_l}{D_l} \left(1 - \frac{1}{W_l G_l} \frac{\partial T}{\partial t} \bigg|_0 \right) . \tag{60}$$

If the surface temperature does not change with time the value of the term in parentheses is 1. For a transient, however, $\partial T / \partial t < 0$, and this term is greater than 1. To account for these transient effects in an approximate way we introduce a parameter f defined by

$$\frac{1}{G_l} \frac{\partial^2 T_l}{\partial z^2} \bigg|_0 = -f \frac{W_l}{D_l} , \tag{61}$$

and we shall present results for $f = 1$ (steady case) and $f = 2$. (A comment on the choice of this particular value will be made in Sec. VII C for a specific case.) With this definition we have

$$I_l \simeq [W_l/D_l(k - \mu'_l)] \{ 1 - f [W_l/D_l(k - \mu'_l)] \} . \tag{62}$$

We show in Fig. 3 the growth rate σ of the instability as a function of the wavenumber k for a vapor velocity $W_v = 10^3$ cm/sec, corresponding to a mass flow rate $J = 0.564$ g/cm² sec. This value is large, but lower than the estimates of Shepherd and Sturtevant.[8] The mass fluxes in the experiment by Fauske and Grolmes[3] can also be estimated to be of this order. The existence of a fastest growing wavelength is obvious from the figure. As $k \to 0$, σ is found to tend to a well-defined positive value. This feature is a consequence of the approximation made in (59), which is not expected to be good for small k. For k greater than the maximum, σ decreases more and more rapidly until the roots of the characteristic equation become complex. This change is indicated by the discontinuity in slope of the continuous lines in Fig. 3, which represent the real part of the root, and by the simultaneous appearance of the dashed lines which show the imaginary part. Further increase of the wavenumber eventually leads to a change in sign of the real part which indicates stability. As indicated above, the present theory is not applicable beyond this point.

Surface transient cooling, as described by the parameter f, is seen to increase the instability. For larger mass fluxes, however, we found an increase in σ for small k but a decrease for large k. The dash-and-dot lines in Fig. 3 have been obtained by approximating the characteristic equation (53) by $S_1 = 0$. As was remarked earlier, this approximation is equivalent to the assumption that the temperature of the liquid–vapor interface does not change due to the presence of the surface wave. The approximate results are very close to the exact ones for the cases of the figure, but the difference increases with increasing vapor velocity as could be expected.

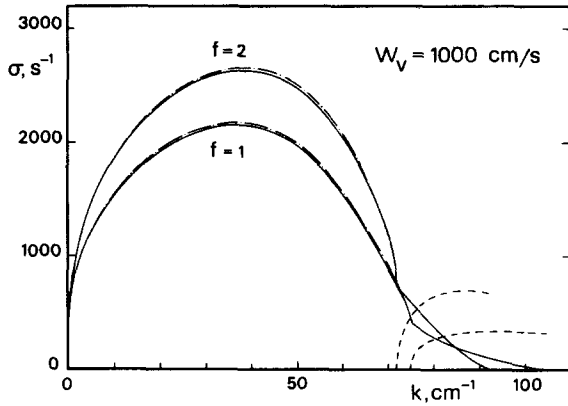In Fig. 4, curve a, the growth rate σ_M of the fastest

FIG. 3. The growth rate of the instability $\sigma(\text{sec}^{-1})$ is shown as a function of the wavenumber k (cm^{-1}) for the parabolic temperature distribution of Sec. VII A. The solid lines are the real part of σ and the dashed lines the imaginary part. The dash-and-dot lines are obtained from the approximation (55) which neglects surface temperature variations. The lower set of curves is for the value $f = 1$ of the parameter defined in (61), the upper set for $f = 2$. The undisturbed vapor velocity is $W_v = 10^3$ cm/sec, corresponding to a mass flux $J = 0.564$ g/cm^2 sec.

FIG. 5. The wavenumber k_M(cm^{-1}) corresponding to the fastest growing wave is shown as a function of the undisturbed vapor velocity W_v(cm/sec) for the parabolic temperature distribution of Sec. VII A (solid line). The dashed line shows the value of k at which σ becomes complex, and the dash-and-dot line the value at which Re σ vanishes.

growing wavelength is shown as a function of the vapor velocity W_v for the case $f = 1$. The growth rate is very small for $W_v < 150$ cm/sec, but increases very rapidly and $\sigma_M^{-1} \simeq 1$ msec at $W_v \simeq 700$ cm/sec, which corresponds to a mass flux $J \simeq 0.40$ g/cm^2 sec. The wavenumber k_M corresponding to the fastest growing wavelength is shown in Fig. 5 as a function of W_v (continuous line). The dashed line in this figure shows the value of k at which the growth rate σ becomes complex, and the dash-and-dot line the value at which Re σ becomes negative (we have not computed this curve for $W_v < 100$ cm/sec). For the reasons already explained the rapid decrease of k_M with W_v renders these results unrealistic for small velocities.

It is now possible to estimate the error introduced by the neglect of viscous effects. As was already remarked, we expect that at not too short wavelengths the only effect of viscosity would be a damping of the interfacial wave. Since vorticity is confined to the vapor, which has a much smaller
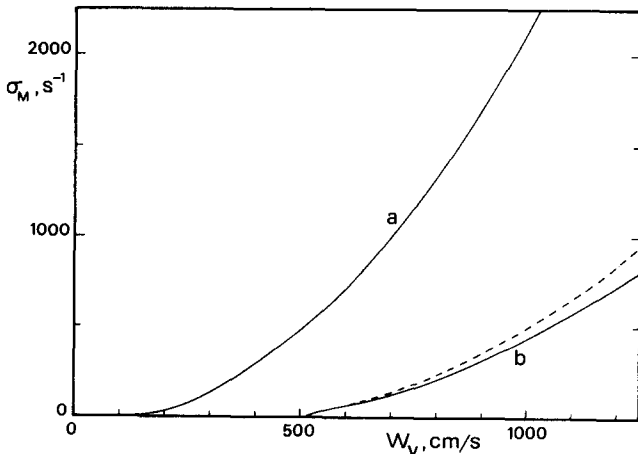
viscosity than the liquid, we may estimate this rate of damping by means of the usual theory of irrotational waves which, for small kinematic viscosities, leads to a value $2\nu k^2$.[29] For $W_v = 10^3$ cm/sec the maximum of σ occurs for $k \simeq 35.5$ cm^{-1}. With $\nu = 2.9 \times 10^{-3}$ cm^2/sec, which is the kinematic viscosity of water at 100 °C, we then find $2\nu k^2 \simeq 7.4$ sec^{-1} which is totally negligible compared with the fastest growth rate $\sigma_M \simeq 2150$ sec^{-1} predicted for this case.

B. Steady case

As a second example we take the steady temperature distribution (16). For the reasons already indicated in Sec. III this distribution does not correspond to conditions readily encountered in nature far from the critical point. However, it is the only case in which our normal mode technique is exact, and the same distribution has been used in the past for the analysis of the same problem.[9] Furthermore, it is clear from the form (49) of I_l that this quantity is influenced essentially by the temperature distribution near the interface. Hence, even if we cannot trust the steady distribution (16) all the way to $z \rightarrow -\infty$, we can use it to represent a thin superficial boundary layer.

In this case the integral I_l has the value

$$I_l = W_l/D_l(k + \mu_l),\tag{63}$$

whereas the second derivative at the interface is given by (61) with $f = 1$.

Figure 6 shows the growth rate σ as a function of the wavenumber for $W_v = 1000$, 1500, and 1900 cm/sec. The corresponding mass fluxes are 0.564, 0.822, and 1.02 g/cm^2 sec. The very rapid growth of the instability with W_v is apparent from this figure, as well as from Fig. 4, curve b, where the maximum growth rate is shown as a function of W_v. The large influence that the temperature profile has on the instability is apparent upon comparing Fig. 3 with Fig. 6 and curves a and b of Fig. 4. Qualitatively the two temperature profiles differ most markedly in the rate of change of the liquid temperature as the free surface is approached, with the previous one giving a more gradual transition as compared to the present exponential one which provides a more rapid

FIG. 4. The growth rate $\sigma(\text{sec}^{-1})$ of the fastest growing wave is shown as a function of the undisturbed vapor velocity W_v(cm/sec) for the parabolic temperature distribution of Sec. VII A with $f = 1$ (curve a) and for the exponential distribution of Sec. VII B (curve b). The dashed line is the result given by the approximation (68) in the latter case.
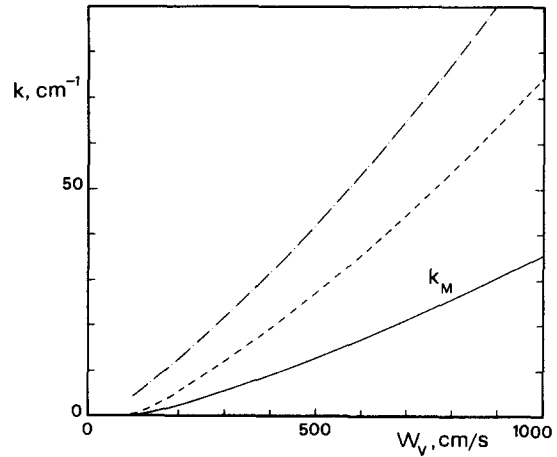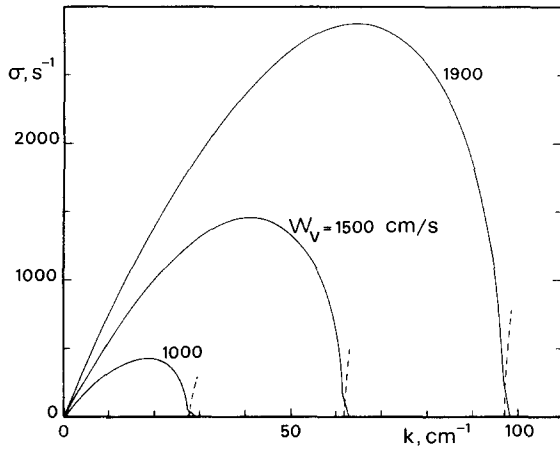
FIG. 6. The growth rate of the instability $\sigma(\sec^{-1})$ is shown as a function of the wavenumber k (cm^{-1}) for the exponential temperature distribution of Sec. VII B. The solid lines are the real part of σ and the dashed lines the imaginary part. The three sets of curves are for $W_v = 1000$, 1500, and 1900 cm/sec.

temperature drop. The thinner boundary layer results in a narrower range of unstable wavenumbers and in smaller growth rates. For the present purposes these two distributions may be expected to be representative of the range of temperature distributions that can be encountered in practice. In this case also, the growth rate σ turns complex and eventually Re σ becomes negative with increasing k. The imaginary part of σ is indicated by the dashed lines in Fig. 6.

The scale of Fig. 6 makes it impossible to show the detailed behavior of σ for small k. It should be observed, however, that in this case σ becomes positive for a finite value of k, which decreases as W_v increases. This is the only case which we have found in which σ is real and goes through zero at the onset of instability. The approach of Palmer[10] is justified only in this situation.

Figure 7 shows as functions of W_v the value of the wavenumber corresponding to the fastest growing wavelength (middle continuous line), the values of k at which the growth rate of the instability becomes complex (upper continuous
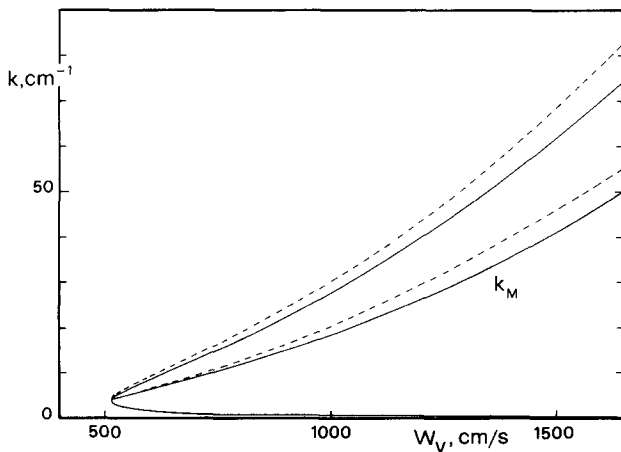

FIG. 7. The wavenumber k_M(cm^{-1}) corresponding to the fastest growing wave is shown as a function of the undisturbed vapor velocity W_v(cm/sec) for the exponential temperature distribution of Sec. VII B (middle solid line). The upper solid curve marks the values of k at which σ becomes complex and the lower solid line the small k instability boundary at which $\sigma = 0$. The dashed lines correspond to the approximations (67) and (69). Note the existence of a threshold value of the vapor velocity in this case.

line), and the lower instability boundary (lowest continuous line). Upon comparison with Fig. 5 this figure clearly shows the reduced instability range of the steeper exponential profile. The existence of a threshold at $W_v \simeq 530$ cm/sec is also apparent from this figure.

For the temperature profile considered here an accidental simplification of the form of S_1 takes place, since it is readily seen that, with (63), Eq. (52) can be written as

$$S_1 = (1 - I_l)[(\rho_l + \rho_v)(\sigma^2 + \omega_0^2) - k^2 J(3W_v - W_l)] .$$
(64)

If now the characteristic equation is approximated by $S_1 = 0$, we find

$$\sigma = \{ [(3W_v - W_l)/(\rho_l + \rho_v)] Jk^2 - \omega_0^2 \}^{1/2} ,$$
(65)

or, neglecting for simplicity ρ_v relative to ρ_l,

$$\sigma \simeq [3(\rho_v/\rho_l)W_v^2 k^2 - \omega_0^2]^{1/2} .$$
(66)

This particularly simple form enables one to obtain an explicit expression for the fastest growing wavenumber k_M:

$$k_M = \frac{JW_v}{\zeta} + \left[\left(\frac{JW_v}{\zeta}\right)^2 - \frac{\rho_l g}{3\zeta}\right]^{1/2} ,$$
(67)

and for the corresponding growth rate

$$\sigma_M = [k_M(k_M W_v W_l - \tfrac{2}{3}g)]^{1/2} .$$
(68)

The dashed lines in Figs. 7 and 4 show these two relations. It is clear that, as in the previous case, the relation $S_1 = 0$ gives a good approximation to the complete characteristic equation. It is also clear from (65) that, for a given W_v, a minimum and a maximum value of k exist for which Re $\sigma > 0$. This range of unstable wavenumbers is given by $k_1 \leqslant k \leqslant k_2$, where

$$k_{1,2} = \frac{3JW_v}{2\zeta} \pm \left[\left(\frac{3JW_v}{2\zeta}\right)^2 - \frac{\rho_l g}{\zeta}\right] .$$
(69)

The value of k_2 given by this formula is shown by the upper dashed line in Fig. 7. The value of k_1 cannot be distinguished from the value given by the complete equation (lowest continuous curve) on the scale of the figure. It is also evident from (69) that a minimum value of the vapor velocity exists for which there is a range of unstable wavenumbers. This value is a threshold for the instability and is given by

$$W_{v,th} = \left(\frac{2}{3}\frac{\rho_l}{\rho_v}\right)^{1/2} \left(\frac{\zeta}{\rho_l}g\right)^{1/4} .$$
(70)

For water at 100 °C this relation gives $W_{v,th} = 527$ cm/sec.

C. A transient temperature distribution

As was already observed, the present analysis can be applied to a nonsteady unperturbed situation only by treating the unperturbed temperature distribution as parametrically dependent on time. This procedure is justified when the time scale for the development of the instability is much shorter than that for the change in time of the unperturbed state.

As an example of the results that can be obtained in the transient case we consider the transient which leads to the steady temperature distribution considered in Sec. VII B. The unperturbed state is therefore specified as follows: a liquid at uniform temperature T_∞ is at rest and occupies the

region $z < 0$; at time $t = 0$ the liquid starts evaporating at a fixed rate, and at the same time it starts moving towards the interface at a velocity $W_l = J/\rho_l$ so that the free surface remains fixed at $z = 0$.

The unperturbed temperature distribution in the liquid is readily obtained by means of the Laplace transform. In particular the temperature gradient is found to be

$$\mathscr{L}\left(\frac{\partial T_l}{\partial z}\right)$$

$$= -s^{-1}G_l \exp\left\{\left[\frac{W_l}{2D_l} + \left(\frac{W_l^2}{4D_l^2} + \frac{s}{D_l}\right)^{1/2}\right]z\right\},$$

where $\mathscr{L}(...)$ denotes the transformed function and s is the transformed variable conjugate to time. Inserting this expression into the definition of I_l, Eq. (49), carrying out the integration with respect to z, and inverting the transform, we find

$$I_l = 2(1 - \beta^2)^{-1/2}(\mathrm{erf}\,\tau^{-1/2}$$

$$+ \beta\left\{\mathrm{erfc}\left(\beta\tau^{1/2}\right)\exp\left[(\beta^2 - 1)\tau\right] - 1\right\}), \quad (71)$$

where

$$\beta = \frac{2D_l}{W_l}\left\{k + \left[\left(\frac{W_l}{2D_l}\right)^2 + k^2 + \frac{\sigma}{D_l}\right]^{1/2}\right\},$$

and the dimensionless time

$$\tau = (W_l^2/4D_l)\,t,$$

has been introduced. An explicit result for the second derivative of T_l can also be obtained which, upon comparison with (61), shows that

$$f = \tfrac{1}{2}[1 + \mathrm{erf}\,\tau^{1/2} + (\pi\tau)^{-1/2}\exp(-\tau)]$$

in this case. It is readily verified that for $\tau \to \infty$, (71) reduces to (63) and f decreases monotonically from infinity to 1. The value $f = 2$ is attained quite rapidly for $\tau \simeq 3.5 \times 10^{-2}$, after which the decrease is much slower. For instance, for $\tau = 0.1$, $f = 1.480$ and for $\tau = 1$, $f = 1.025$. The value $f = 2$ used in the first example is seen here to be representative of conditions at the end of the very rapid initial transient.
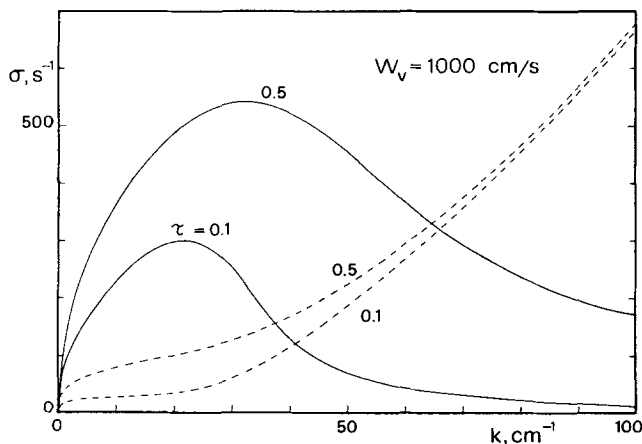
In Fig. 8 we show the growth rates obtained for this case for $\tau = 0.1$, 0.5 and in Fig. 9 those for $\tau = 1$, 1.5 and $\tau \to \infty$ for $W_v = 1000$ cm/sec. In these figures the real part of σ is shown by the continuous lines, whereas Im σ is indicated by the dashed lines. A marked change in behavior is apparent from these results. For small τ (Fig. 8), σ is complex for all values of k, which corresponds to an oscillating surface wave of growing amplitude; whereas, for increasing τ a larger and larger interval of wave numbers in which σ is real appears. The curve corresponding to steady conditions is approached very rapidly. The maximum growth rate at first decreases with increasing τ, and then starts to increase once the corresponding value of σ becomes real. The range of unstable wavenumbers is seen to decrease with increasing time, and the fastest growing wavelength remains in the range 15–35 cm^{-1} for all times. It may be noted that the present model, in which time enters only parametrically, predicts instability for all values of τ.

D. Thermodynamic equilibrium assumption

As was indicated in Sec. VI, the assumption that the vapor pressure at the liquid surface coincides with that prescribed by local thermodynamic equilibrium results in a different characteristic equation from the one used to obtain the results discussed thus far. In Fig. 10 we show a comparison between the results obtained by means of this assumption with the previous ones. The case considered is that of Fig. 3 for $f = 1$, i.e., the approximation (62) has been used for I_l, the relation (61) for $\partial^2 T/\partial z^2$, and $W_v = 1000$ cm/sec. The thermodynamic equilibrium results are shown by the curves marked a and those of Fig. 3 by the ones marked b. The qualitative behavior is very similar although there is some quantitative difference. These results confirm the fact that surface temperature changes have only minor effects on the instability studied here.
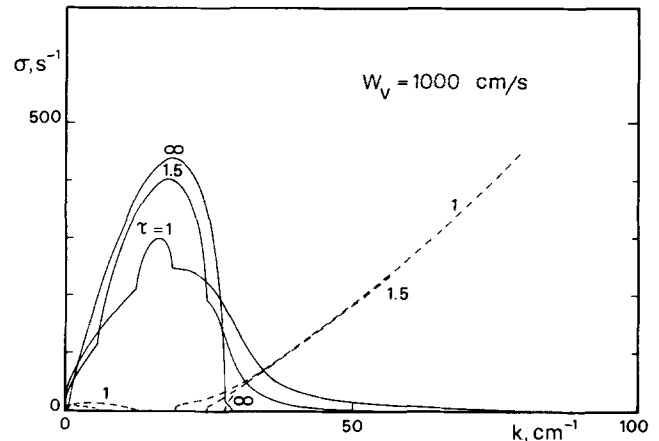

FIG. 8. The growth rate of the instability $\sigma(\sec^{-1})$ is shown as a function of the wavenumber k (cm^{-1}) for the time-dependent case of Sec. VII C for $\tau = 0.1$ and $\tau = 0.5$. The solid lines are the real part of σ and the dashed lines the imaginary part. The undisturbed vapor velocity has the value $W_v = 1000$ cm/sec.

FIG. 9. The growth rate of the instability $\sigma(\sec^{-1})$ is shown as a function of the wavenumber k (cm^{-1}) for the time-dependent case of Sec. VII C for $\tau = 1$, $\tau = 1.5$, and $\tau \to \infty$. These last results are the same as those shown in Fig. 6. The solid lines are the real part of σ and the dashed lines the imaginary part. The undisturbed vapor velocity has the value $W_v = 1000$ cm/sec.
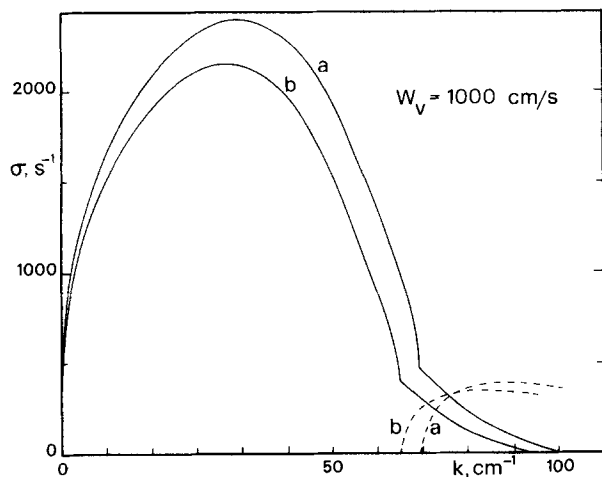
FIG. 10. Comparison between the results obtained by imposing thermodynamic equilibrium at the interface (curves a) with those of Fig. 3 (curves b). The solid lines are the real part of the instability growth rate σ and the dashed lines are the imaginary part. The temperature distribution is the parabolic one of Sec. VII A and the value of the undisturbed vapor velocity is $W_v = 1000$ cm/sec.

E. The effect of vapor vorticity

As a final point it is of interest to inquire about the effect of vorticity in the vapor on the stability of the interface. The problem can be solved by the same procedure under the assumption of irrotational motion in the vapor if the requirement of continuity of tangential velocity at the interface is dropped. Rather than writing down the general result we consider only the exponential steady profile of Sec. VII B which leads to particularly simple expressions. In this case, the term $(1 - I_t)$ can be factored out from S_1 as in Eq. (64) and the remaining expression equated to zero to approximate the complete characteristic equation. The result is

$$(\rho_l + \rho_v)\sigma^2 - 2kJ\sigma + (\rho_l + \rho_v)\omega_0^2 - k^2 J(W_v - W_l) = 0,$$

from which, using the approximation $\rho_v \ll \rho_l$,

$$\sigma \simeq kW_l + [k^2(\rho_v/\rho_l)W_v^2 - \omega_0^2]^{1/2}.$$

The first term is always positive, but the predicted growth rate, measured on the time scale ω_0^{-1}, is exceedingly small and hence can be disregarded. The remaining term is then to be compared with the previous result (66) obtained by means of the analogous approximations. It is seen that the effect of the vapor vorticity is to increase the coefficient of the first term in the square root from 1 to 3. We conclude therefore that vorticity does have a destabilizing effect, but that it cannot account in full for the instability that we have described. Furthermore, the fact that the presence of vorticity does not add new terms to the characteristic equation but merely changes the numerical value of a coefficient seems to imply that the instability has its roots in other phenomena, the effect of which is only amplified by the vapor vorticity. We have already described the nature of these phenomena in Sec. IV.

VIII. CONCLUSIONS

The theoretical results obtained in this study depend on the unperturbed temperature distribution near the interface which is not known. This circumstance has prevented us from effecting a comparison with experiment. For the same reason it has not been possible to reach conclusions of general validity. However, on the basis of several different temperature distributions, it has been found that the surface of a rapidly evaporating liquid can become unstable for a range of wave numbers. At large mass fluxes the instability is quite violent, with characteristic growth times of a millisecond or less.

It has been found that in all the cases investigated the results can be well approximated by assuming that the liquid surface temperature is not affected by the perturbation. This observation seems to imply that the most important element in the development of the instability is the change in mass flux caused by the change in temperature gradient at the interface. When a surface wave is present, the flux from the (liquid) crests where the thermal boundary layer is stretched, decreases and that from the troughs, where the boundary layer is compressed, increases. Since the vapor leaving the surface pushes back on the liquid due to the increase in specific volume, the consequence is that the pressure in the liquid is increased at the troughs relative to the crests, so that the liquid is squeezed into the crests and causes their growth (Fig. 2). A corresponding deepening of the troughs also takes place at the same time. This mechanism is contrary to that termed "fluid inertia" by Palmer,[10] which requires the pressure in the liquid troughs to decrease. We have not found evidence of this behavior in any of the cases examined. Evidence for Palmer's "differential vapor recoil" mechanism has also not been found, at least to the extent that it is caused primarily by local surface temperature variations. The "moving boundary" mechanism, if it exists, seems to be of very minor importance. The mechanism that we have found is similar in its action to the "differential vapor recoil" one, but in its origin it is rather akin to the "moving boundary" one and therefore it cannot be identified with either one of them. The other two mechanisms described by Palmer depend on viscosity and surface tension gradients, both of which we have neglected in the present mathematical model. It may also be noted that under conditions of marginal stability (i.e., when the real part of the growth rate vanishes) the imaginary part does not necessarily vanish. Hence, applicability of the principle of exchange stability on which the work of Palmer is based should not be taken for granted in the present problem.

ACKNOWLEDGMENTS

APPENDIX: SOLUTION OF THE PERTURBATION PROBLEM

We outline here the method and the essential steps leading to the solution of the perturbation problem given in Sec. V.

Upon taking the curl of the momentum equation (23) we find

$$\left(\frac{\partial}{\partial t} + W\frac{\partial}{\partial z}\right)\omega = 0, \quad (A1)$$

where ω denotes the vorticity. This equation implies that ω depends on z and t only through the combination $t - z/W$. It can be shown that ω can be expressed as[30]

$$\omega = \nabla\times[A\,\mathbf{K} + \nabla\times(B\,\mathbf{K})]. \quad (A2)$$

Since $\omega = \nabla\times\mathbf{u}'$, this relation implies that

$$\mathbf{u}' = A\,\mathbf{K} + \nabla\times(B\,\mathbf{K}) + \nabla\varphi, \quad (A3)$$

where, from the equation of continuity, φ must satisfy

$$\nabla^2\varphi = -\frac{\partial A}{\partial z}. \quad (A4)$$

Upon substitution of (A3) into (23), in view of the dependence of A and B on the variable $t - z/W$, we find

$$p' + \rho\left(\frac{\partial\varphi}{\partial t} + W\frac{\partial\varphi}{\partial z}\right) = 0. \quad (A5)$$

The general solution of (A4) is readily determined to be

$$\varphi = \left(P_0(t)f - \frac{1}{2}\int_0^z e^{-kz}A\,dz\right)e^{kz}$$
$$+ \left(Q_0(t)f - \frac{1}{2}\int_0^z e^{kz}A\,dz\right)e^{-kz}, \quad (A6)$$

from which, upon substitution into (A5) and use of the relation $\partial A/\partial t = -W\,\partial A/\partial z$, the following expression for the pressure field is obtained:

$$p' = \rho\{[(kWQ_0 - \dot{Q}_0)f - \tfrac{1}{2}WA(x,y,0,t)]e^{-kz}$$
$$- [(\dot{P}_0 + kWP_0)f - \tfrac{1}{2}WA(x,y,0,t)]e^{kz}\}, \quad (A7)$$

where the dots denote time differentiation.

These results are general and do not involve any assumption on the time dependence of the various quantities. We now adapt them to the liquid field. For an exponential time dependence (A1) gives

$$A_l = \alpha_l f(x,y)\exp[\sigma(t - z/W_l)].$$

Since Re $\sigma > 0$ in the unstable case, and since $z < 0$ in the liquid, it is necessary that $\alpha_l = 0$ for A_l to be bounded at infinity. Similarly, one finds $B_l = 0$ and, from the requirement of boundedness of $\varphi_l, Q_{0l} = 0$. Thus, the motion in the liquid is irrotational and (A6) and (A7) give, after a renaming of the constants, Eqs. (31) and (35) for φ_l and p'_l, respectively.

For the vapor field we have

$$A_v = \alpha_v f(x,y)\exp[\sigma(t - z/W_v)], \quad (A8)$$

whereas boundedness of φ_v for $z\to\infty$ requires that

$$P_{0v}(t)f = \frac{1}{2}\int_0^\infty e^{-kz}A_v\,dz$$

or

$$P_{0v} = \tfrac{1}{2}[\alpha_v/(k + \sigma/W_v)]e^{\sigma t}.$$

With these expressions it is readily seen that (33) and (36) are obtained for the vapor field.

Continuity of the tangential velocity requires that on $z = 0$,

$$\varphi_l - \varphi_v = (W_v - W_l)\eta,$$
$$B_l = B_v.$$

The first relation allows one to express α_v in terms of Φ_l, Φ_v, and a, while the second one implies $B_v = 0$.

We turn now to the energy equations (24). Setting

$$T' = \theta(z)f(x,y)e^{\sigma t}, \quad (A9)$$

the perturbed energy equation in the vapor becomes

$$D_v\frac{d^2\theta_v}{dz^2} - W_v\frac{d\theta_v}{dz} - (D_v k^2 + \sigma)\theta_v = 0, \quad (A10)$$

since the undisturbed temperature gradient vanishes in the vapor. The solution of this equation bounded for $z\to\infty$ is

$$\theta_v = \Theta e^{-\mu v_z}, \quad (A11)$$

where μ_v is given by (48) and Θ is the (total) temperature perturbation at the interface. The presence of an unperturbed gradient renders the liquid energy equation more complex, namely

$$D_l\frac{d^2\theta_l}{dz^2} - W_l\frac{d\theta_l}{dz} - (D_l k^2 + \sigma)\theta_l = k\Phi_l e^{kz}\frac{\partial T_l}{\partial z}. \quad (A12)$$

For general $\partial T_l/\partial z$ the solution of this equation bounded for $z\to\infty$ can be obtained by Lagrange's method of variation of constants and may be written

$$\theta_l = \left(\Theta + \frac{1}{\mu_l - \mu'_l}\int_{-\infty}^0 e^{-\mu'_l z}F_l(z)dz\right.$$
$$+ \frac{1}{\mu_l - \mu'_l}\int_0^z e^{-\mu'_l z}F_l(z')dz' - a\left.\frac{\partial T_l}{\partial z}\right|_0\right)e^{\mu_l z}$$
$$+ \frac{1}{\mu'_l - \mu_l}e^{\mu'_l z}\int_{-\infty}^z e^{-\mu'_l z'}F_l(z')dz', \quad (A13)$$

where μ_l and μ'_l are given by (47) and (50) and we have set $F_l = k\Phi_l D_l^{-1}\partial T_l/\partial z\,e^{kz}$ for brevity. The remaining integration constant in (A13) has been written in such a way that, if due account is taken of the unperturbed temperature gradient, Θ is the perturbation of the interface temperature. From (A13) the expression (45) for the perturbed temperature gradient at the interface is obtained, which completes the solution.

It may be noted that in the stable case Re $\sigma < 0$ and one would find $\alpha_v = 0$, $\alpha_l \neq 0$ and the vorticity would be confined to the liquid.

[1] A. R. Edwards and T. P. O'Brien, J. Br. Nucl. Energy Soc. **9**, 125 (1970).
[2] J. H. Lienhard, M. Alamgir, and M. Trela, J. Heat Transfer **100**, 473 (1978).
[3] H. K. Fauske and M. S. Grolmes, in Proceedings of the Fifth International Heat Transfer Conference, Tokyo, 1974, Vol. 4, p. 30.
[4] F. C. Hooper and P. S. K. Luk, in Ref. 3, p. 70.
[5] K. Hickman, Ind. Eng. Chem. **44**, 1892 (1952).
[6] K. Hickman, J. Vac. Sci. Technol. **9**, 960 (1972).
[7] H. J. Palmer and J. C. Maheshri, Int. J. Heat Mass Transfer **24**, 117 (1981).
[8] J. E. Shepherd and B. Sturtevant, J. Fluid Mech. **121**, 379 (1982).
[9] C. A. Miller, AIChE J. **19**, 909 (1973).

[10]H. J. Palmer, J. Fluid Mech. **75**, 487 (1976).

[11]J. C. Maheshri and H. J. Palmer, AIChE J. **25**, 183 (1979).

[12]L. D. Landau and E. M. Lifshitz, *Fluid Mechanics* (Pergamon, New York, 1959).

[13]D. Y. Hsieh, J. Basic Eng. **87**, 981 (1965).

[14]D. Y. Hsieh, J. Basic Eng. **94**, 156 (1972).

[15]A. Prosperetti, Meccanica **14**, 34 (1979).

[16]V. G. Levich, *Physicochemical Hydrodynamics* (Prentice–Hall, Englewood Cliffs, NJ, 1962), p. 384.

[17]C. S. Yih, *Fluid Mechanics* (McGraw–Hill, New York, 1969), p. 461.

[18]S. Ostrach, in *Physicochemical Hydrodynamics, V. G. Levich Festschrift*, edited by D. B. Spalding (Advance Publications, London, 1977), Vol. 2, p. 571.

[19]S. M. Pimputkar and S. Ostrach, Phys. Fluids **23**, 1281 (1980).

[20]E. H. Kennard, *Kinetic Theory of Gases* (McGraw–Hill, New York, 1938), Chap. III.

[21]R. W. Schrage, *A Theoretical Study of Interphase Mass Transfer* (Columbia U. P., New York, 1953).

[22]A. F. Mills, Int. J. Multiphase Flow **6**, 41 (1980).

[23]L. D. Koffman, M. S. Plesset, and L. Lees, submitted to Phys. Fluids.

[24]M. S. Plesset, J. Chem. Phys. **20**, 790 (1952).

[25]M. S. Plesset and A. Prosperetti, J. Fluid Mech. **78**, 433 (1976).

[26]E. G. Mahler, R. S. Schechter, and E. H. Wissler, Phys. Fluids **11**, 1901 (1968).

[27]L. D. Landau, Acta Physicochim. URSS **19**, 77 (1944).

[28]T. R. Goodman, in *Advances in Heat Transfer*, edited by T. F. Irvine and J. P. Hartnett (Academic, New York, 1964), Vol. 1, p. 51.

[29]H. Lamb, *Hydrodynamics* (Cambridge U.P., Cambridge, 1932; reprinted by Dover, New York, 1945).

[30]L. Cortelezzi and A. Prosperetti, Q. Appl. Math. **38**, 377 (1981); **39**, 424 (1981).